

Laser Spectroscopy of Cooled Zirconium Fission Fragments

P. Campbell,¹ H. L. Thayer,² J. Billowes,¹ P. Dendooven,³ K. T. Flanagan,¹ D. H. Forest,² J. A. R. Griffith,² J. Huikari,³ A. Jokinen,³ R. Moore,¹ A. Nieminen,³ G. Tungate,² S. Zemlyanoi,¹ and J. Äystö³

¹*Schuster Laboratory, University of Manchester, Manchester M13 9PL, United Kingdom*

²*School of Physics and Astronomy, University of Birmingham, Birmingham B15 2TT, United Kingdom*

³*Department of Physics, University of Jyväskylä, PB 35 (YFL) FIN-40351 Jyväskylä, Finland*

(Received 3 April 2002; published 5 August 2002)

The first on-line laser spectroscopy of cooled fission fragments is reported. The $^{96-102}\text{Zr}$ ions, produced in uranium fission, were extracted and separated using an ion guide isotope separator. The ions were cooled and bunched for collinear laser spectroscopy by a gas-filled linear Paul trap. New results for nuclear mean-square charge radii, dipole, and quadrupole moments are reported across the $N = 60$ shape change. The mean-square charge radii are found to be almost identical to those of the Sr isotones and previously offered modeling of the radial changes is critically reviewed.

DOI: 10.1103/PhysRevLett.89.082501

PACS numbers: 21.10.Ft, 21.10.Ky, 27.60.+j, 42.62.Fi

The competition between the various, coexisting, nuclear shapes (well-deformed prolate, oblate, or spherical) in the neutron-rich $A \sim 100$ region has been of long-standing nuclear-structural interest and the subject of many nuclear spectroscopic studies [1–3]. Isotopes in this region are abundantly produced in the fission of transuranic elements and such sources have been studied in detailed γ -ray spectroscopy measurements [4,5]. Investigations of the nuclear shape using extremely sensitive and model-independent *optical* spectroscopy has, however, been impossible in the ${}_{39}\text{Y}-{}_{45}\text{Rh}$ region. This is due to the refractory nature of these elements which prevents their efficient production at conventional isotope separator facilities. High-resolution optical studies have thus been restricted to explorations of elements with $Z \leq 38$ [6–12] or naturally occurring, stable isotopes at higher Z . In this Letter, we present the use of a recently developed technique [13], involving the cooling and trapping of radioactive ions, that facilitates the optical study of refractory fission products. We report the first laser spectroscopic measurements on zirconium fission fragments from ${}^{96}\text{Zr}$ to ${}^{102}\text{Zr}$. Nuclear spins, I , magnetic moments, μ , spectroscopic quadrupole moments, Q_s , and changes in nuclear mean-square charge radii, $\delta\langle r^2 \rangle$, are evaluated across the $N = 60$ shape change.

Production of singly charged radioactive ions from fission fragment recoils is achieved at the IGISOL (Ion Guide Isotope Separator On-Line) facility of the University of Jyväskylä Accelerator Laboratory (JYFL) by the use of a flowing gas catcher-thermalizer [14]. The technique shows little sensitivity to the chemistry of the recoiled species and release times are extremely fast, ~ 1 ms, compared to conventional ion sources. The laser spectroscopic station at the IGISOL facility [15] has been recently enhanced by the addition of an on-line cooler-buncher [13]. High-resolution laser spectroscopy has been demonstrated in a study of the odd- N ${}^{175}\text{Hf}$ isotope using ion fluxes as low as $\sim 400 \text{ s}^{-1}$ [13]. A full description of each part of the experimental apparatus: the IGISOL; the laser spectroscopy station; and the cooler-buncher; may be found elsewhere [14–16]. In

brief, high-energy fragments from the proton-induced fission of natural uranium are slowed and thermalized in fast-flowing helium gas. A significant fraction, 1 – 10%, of the thermalized recoils retain a 1^+ charge state in the buffer gas and this fraction is skimmed from the carrier gas (in the jet expansion region) and is injected into an isotope separator. Following acceleration and mass analysis the fission fragments are slowed and injected into the JYFL cooler-buncher [16]. The cooler-buncher, a gas-filled linear Paul trap on a 40 kV platform, provides efficient storing and cooling of the ions and, on opening the trap, is capable of delivering low-emittance (3π mm mrad), low energy spread (< 0.6 eV) ionic ensembles in bunches of $\sim 15 \mu\text{s}$ duration. The device can be held at an extremely precise constant voltage, $< \pm 0.1$ V in 40 kV, for long time periods, of order days. The reaccelerated bunches are electrostatically transported to a laser spectroscopy station [15]. At this point the ionic ensemble is formed into a low-divergence narrow beam and is overlapped with a counter-propagating laser beam from a frequency-doubled Spectra Physics 380D dye laser locked to an I_2 absorption line. An 18 mm length of the overlap region is imaged, via a quartet of fused-silica lenses, onto a Hamamatsu R5900P-03-L16 photomultiplier. The photomultiplier is gated to register only photons while the ion bunch traverses the imaged region (providing $\sim 10^4$ suppression of the photon background). For the zirconium experiment the ionic ground state transition $d^2s^4F_{3/2} - d^2p^4F_{5/2}$ (327 nm) was Doppler tuned to resonance with a fixed laser frequency of $30\,523.3494 \text{ cm}^{-1}$.

Although the zirconium system is a chemical homolog of hafnium, the first cooler test case [13], it does not share the same ionic ground state ($ds^2^2D_{3/2}$ in Hf). The structure of the ionic ground state influences both the choice of resonance transition and the ion survival time (chemical reaction rate) in the cooler-buncher. Optimization of cooling and bunching times were investigated off-line, using a Zr discharge source, and again during the fission experiment. The zirconium radioactivity was observed to

survive storage for periods of order seconds without loss. The activity was monitored using both a gamma-ray counting station and the β -activity buildup on a microchannel plate detector positioned downstream of the laser interaction region [17]. Despite zirconium activity being observed during the longer storage times, significant losses in spectroscopic efficiency were incurred for any storage period greater than 200 ms. These losses were identified, off-line, as resulting from the formation of charged zirconium complexes in the cooler-buncher. Identification was achieved using the path from the cooler-buncher to photomultiplier and channelplate detectors as a time-of-flight (TOF) spectrometer. TOF spectra were taken for *all* ions in the ensemble, using the channelplates, and fluorescent ions *alone* by timing the detection of resonantly scattered photons (shown in Fig. 1).

In comparison to the fluorescent ion spectrum, which shows the native ion content of the ensemble, the total ion output of the cooler-buncher is observed to contain increasing amounts of charged molecules with increasing storage time. The molecules are believed to be $Zr^+(H_2O)_n$ complexes compatible with the TOF spectra and known impurities in the buffer gas. During the on-line experiment the cooler-buncher was continuously loaded for 200 ms periods, before releasing the bunched sample, in order to optimize the signal to background.

Neutron-rich zirconium nuclei, $^{96-102}Zr$, were produced by the fission of uranium, induced using $3.5 \mu A$ of 25 MeV H^+ . A production of ~ 3000 ions per second was achieved (after cooling) for the most strongly produced, ^{100}Zr , isotope. Minimum ion rates of ~ 500 ions

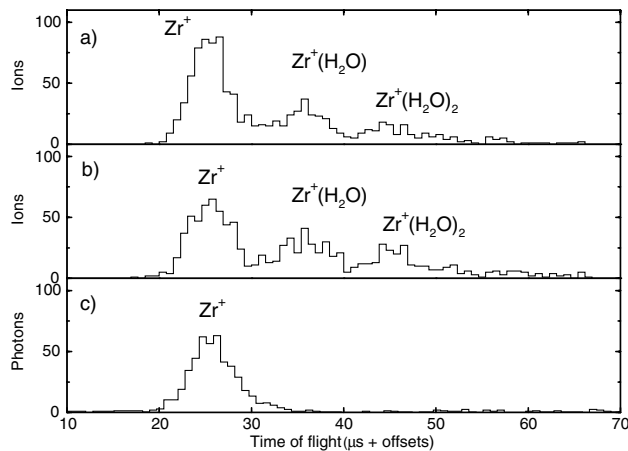


FIG. 1. Normalized ion and fluorescent ion time-of-flight spectra taken using 10^3 ^{96}Zr ions per bunch (injected within 10 ms) and stored for (a) 100 ms and (b),(c) 150 ms. The spectra are offset by $70 \mu s$ total flight time and spectrum (c) is further corrected by $\sim 4 \mu s$ corresponding to the path difference from photomultiplier to channelplate detector. Ion bunches in spectra (a) and (b) are observed to arrive at times corresponding to masses 96, ~ 114 , ~ 132 (and heavier) and are assigned to $Zr^+(H_2O)_n$ complexes.

per second were studied on the more weakly produced isotopes (particularly ^{96}Zr). The full hyperfine structure was observed for all isotopes with the exception of the weakest component in the $I^\pi = 1/2^+$ structure of $^{97,99}Zr$.

Figure 2 shows a photon spectrum for ^{100}Zr as a function of total acceleration voltage. A systematic uncertainty is encountered in the determination of the voltage. In absolute terms the cooler voltage and tuning voltages are determined to an accuracy of 0.01%, with the cooler voltage read in a 1 : 10 000 division of a 1000 M Ω resistive stack. Differential changes in resonance voltages between isotopes can be determined to far higher precision, typically $\Delta V \sim \pm 0.1$ V. The uncertainty in absolute laser frequency determination gives a comparable systematic uncertainty, but the differential error (± 2 MHz) is again small. Drifts, primarily changes in laser frequency, incurred during experimental periods are corrected by measuring with regular reference to a calibration isotope (^{100}Zr in this case). In Fig. 2, eight scans of 17 min duration, taken intermittently during an 11 h period, are shown in simple summation. Figure 3 shows an experimental spectrum for ^{101}Zr (converted to frequency) that contains the summation of two blocks of data, of 16 and 8 h duration taken 60 h apart. The summation is corrected for a change in laser locking frequency that resulted in a centroid shift equivalent to 1.6 V. Negligible drift was observed in voltage or laser frequency during the acquisition of either of the blocks of measurements themselves. Figure 3 also shows the two best fits, for $I = 3/2$ and $5/2$, to the hyperfine structure. The nuclear spin of ^{101}Zr was determined to be $I = 3/2$ consistent with a suggested spin assignment [18].

Tables I and II show the hyperfine parameters, nuclear spins, and isotope shifts determined in this work (including off-line measurements on the stable zirconium isotopes). Nuclear magnetic moments, quadrupole moments, and changes in mean-square charge radii were extracted from these data. For the changes in mean-square charge radii, $\delta\langle r^2 \rangle$, the combined analysis of Fricke *et al.* [22] and a reanalysis of $\delta\langle r^2 \rangle^{90,91}$ [23] were taken as references. Values for the nuclear mass shift, $\delta\nu^{90,92} = +150(33)$ MHz, and nuclear field shift, $F\delta\langle r^2 \rangle$, where

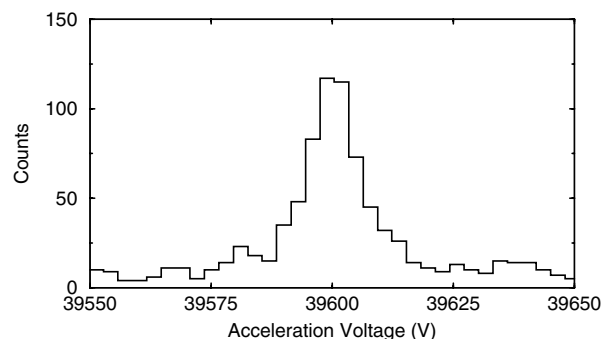


FIG. 2. Resonance fluorescence spectrum for ^{100}Zr taken with ~ 3000 ions per sec and a total accumulation time of 2.27 h.

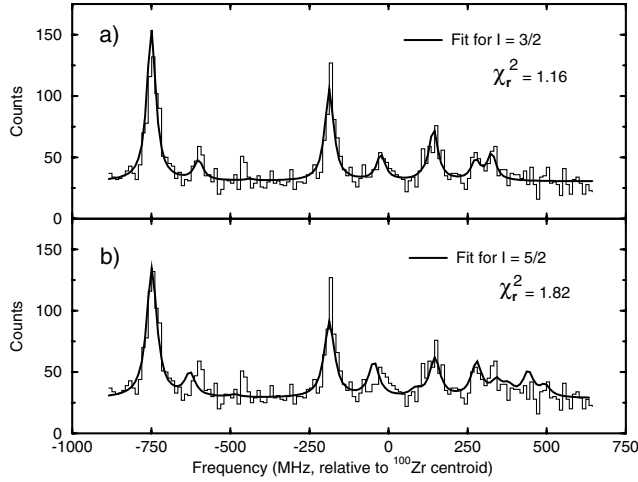


FIG. 3. Resonance fluorescence spectrum for ^{101}Zr taken with ~ 1500 ions per sec and a total accumulation time of 24 h. Voigt profile fits to the data, and reduced χ^2 , are shown for (a) $I = 3/2$, and (b) $I = 5/2$ (with this spin assignment rejected).

$F = -2083(118) \text{ MHz fm}^{-2}$, were also derived from the calibration. The $\sim 5\%$ overall uncertainty assigned to $\delta\langle r^2 \rangle$, directly follows the analysis of Fricke *et al.* [22]. For the nuclear moments, the compilation of Raghavan [19] and the “year-2001” evaluation of $Q_s(^{91}\text{Zr}) = -0.176(3) \text{ b}$ [20] were used to calibrate the moments (with an additional, 1%, uncertainty allowance for the hyperfine anomaly [21]).

Figure 4 shows the zirconium mean-square charge radii as a function of neutron number. The mean-square charge radii are observed to increase steadily with increasing neutron number until the known shape change at $N = 60$ [4]. Beyond the discontinuity at $N = 60$, the increase in $\langle r^2 \rangle$ with neutron number returns to a level comparable to that before the shape change. The change in mean-square charge radius resulting from a change in mean-square multipole deformation, $\delta\langle \beta_i^2 \rangle$, is commonly given to first order, Ref. [26], by

TABLE I. Nuclear spins, hyperfine parameters, magnetic moments, and spectroscopic quadrupole moments determined in the $\text{Zr}^+ d^2 s^4 F_{3/2}$ ground term (and calibration data from other work [19,20]). Hyperfine parameters for the $d^2 p^4 F_{5/2}$ term in $^{97,99}\text{Zr}$ were constrained to be in the ratio individually determined in ^{91}Zr and ^{101}Zr . An additional 1% error, to account for possible hyperfine anomalies, is added to the error assigned to the magnetic moments [21].

A	I	$A(^4F_{3/2})$ (MHz)	$B(^4F_{3/2})$ (MHz)	μ (μ_N)	Q_s (b)
91	5/2	+333.3(3)	-14.7(8)	-1.30362(3) ^a	-0.176(3) ^b
97	1/2	+1197.4(17)		-0.937(11)	
99	1/2	+1189.1(13)		-0.930(10)	
101	3/2	+115.9(4)	+67.8(27)	-0.272(4)	+0.812(56)

^aReference [19]. ^bReference [20].

TABLE II. Isotope shifts in the $\text{Zr}^+ d^2 s^4 F_{3/2} - d^2 p^4 F_{5/2}$ transition and changes in mean-square charge radii (following the calibration data of Refs. [22,23]). Statistical errors are shown in rounded brackets and full systematic errors are denoted by square brackets.

A	Isotope Shift $\nu^{90} - \nu^A$ (MHz)	$\delta\langle r^2 \rangle^{90,A}$ (fm^2)
91	+192(3) [5]	+0.128 [6] ^a
92	+494(3) [7]	+0.310 [16] ^a
94	+823(3) [10]	+0.537 [27] ^a
96	+1033(3) [11]	+0.702 [35] ^a
97	+1198(10) [20]	+0.813(5) [41]
98	+1480(11) [23]	+0.980(5) [49]
99	+1642(9) [22]	+1.089(5) [54]
100	+2759(9) [31]	+1.665(4) [83]
101	+3067(10) [35]	+1.843(5) [92]
102	+3288(11) [37]	+1.979(5) [99]

^aReferences [22,23].

$$\delta\langle r^2 \rangle = \langle r^2 \rangle_s \frac{5}{4\pi} \sum_i \delta\langle \beta_i^2 \rangle,$$

where $\langle r^2 \rangle_s$ is the mean-square charge radius of the corresponding spherical nucleus and i denotes the multipole order. If changes in the measured zirconium mean-square charge radii relative to a spherical droplet model datum

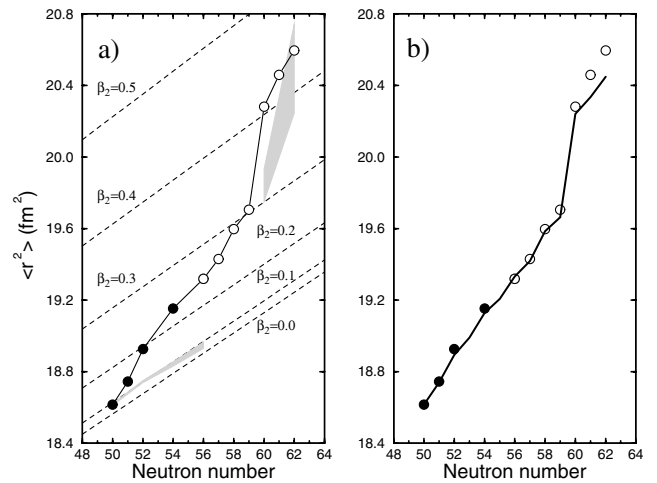


FIG. 4. The zirconium mean-square charge radii as a function of neutron number. Measurements on stable isotopes are shown by the full circles and those on fission fragments by the open circles. A $\sim 5\%$ systematic calibration error on $\delta\langle r^2 \rangle$ is not shown. (a) Droplet model β_2 -isodeformation contours [24] are shown with the experimental data normalized to the reported ^{90}Zr β_2 deformation [25]. Model-dependent mean-square charge radii, derived using β_2 deformations from nuclear lifetime measurements [25], are shown with uncertainties bounded by the shaded regions. (b) A comparison of the zirconium mean-square charge radii with those in the strontium isotones [9,10] (indicated by the solid line). The data are set equal at $N = 50$ and systematic errors are not shown.

[24] are assigned solely to changes in quadrupole deformation then an approximate, model-dependent comparison of trends in $\langle\beta_2^2\rangle$ from optical data can be made with those extracted from $B(E2)$ values, derived from nuclear lifetime measurements [25]. In regions of strong quadrupole deformation, such as that beyond the $N = 60$ shape change, the approximations invoked, namely, that changes in $\langle\beta_2^2\rangle$ dominate the charge radii changes and that the sum $B(E2)$ strength of all excited 2^+ states is dominated by that of the first state, are found to be reliable and consistency between optical measurement and nuclear lifetime measurement is observed (see Fig. 4(a)). For the zirconium isotopes below $N = 58$, however, the approximations are observed to be poor. The level of discrepancy is found to be almost identical to that observed in the neighboring Sr isotope chain [27]. Such discrepancies arise from the approximations made in the extraction of $\langle\beta_2^2\rangle$ from both $\langle r^2 \rangle$ and $B(E2)$.

Mach *et al.* [27] (with reference to Buchinger *et al.* [28]) have considered in detail the discrepancy between charge radii trends and $B(E2)$ trends in the neighboring strontium isotope chain from $N = 40$ –62. As noted, the trends in zirconium and strontium are found to be identical in this work (within the systematic errors). Mach *et al.* concluded for strontium that on the whole the discrepancies between the nuclear parameters would largely be accounted for by the correct inclusion of octupole vibrations and not “missing” $B(E2)$ strength [27]. In zirconium, in the $50 \leq N \leq 56$ transitional region, such a conclusion is unconvincing. The $\langle\beta_3^2\rangle$ parameters evaluated in Ref. [27] could, within model-dependent uncertainties, provide a change in charge radius compatible with that measured for the $^{90,96}\text{Zr}$ pair alone. For other Zr isotopes however, particularly $A = 90$ –94, the changes in $\langle\beta_3^2\rangle$ (and $\langle\beta_2^2\rangle$) wholly fail to explain the observed trends in the mean-square charge radius. The droplet model datum [24], critical to the interpretation, appears accurate with the correct $\delta\langle r^2 \rangle$ increases reproduced in the region close to the saturation of the deformation. Further contributions to $\delta\langle r^2 \rangle$ are therefore present in the transitional region. Recent gamma-ray spectroscopic studies and lifetime measurements in the transitional zirconium region reported by Urban *et al.* [4], particularly those for $^{98,99}\text{Zr}$, have firmly established a steady onset of deformation in the excited rotational structures of zirconium from $N = 58$ to 64. The Authors of Ref. [4] were led, from extrapolations to unobserved 0^+ bandheads, to propose a gradual increase in deformation throughout the transitional region. Such a behavior appears extremely close to that displayed by the course of the mean-square charge radius. As such, it is suggested that the contribution of missing $B(E2)$ strength to $\langle r^2 \rangle$ may well transpire to be more significant than that of $\langle\beta_3^2\rangle$ in both strontium and zirconium.

Predictions of the zirconium ground state deformation and charge radii successfully model the deformed, $N \geq$

60, region but range in their ability to model the transitional region. Relativistic mean-field calculations [29] on the whole reproduce the trends in $\langle r^2 \rangle$ but with too smooth a radial increase at $N = 60$. Global macroscopic-microscopic calculations [30] predict a far sharper shape change, compatible with that observed, but with worse overall agreement.

Further studies of refractory fission fragments are underway at the JYFL IGISOL facility and, in the future, the yttrium isotopes and heavier $^{103-105}\text{Zr}$ isotopes will be investigated.

This work has been supported by the U.K. Engineering and Physical Sciences Research Council, the Academy of Finland under the Finnish Centre of Excellence Programme 2000–2005 (Project No. 44875), and by the European Union Fifth Framework Programme “Improving Human Potential—Access to Research Infrastructure” Contract No. HPRI-CT-1999-00044.

-
- [1] E. Chieftz *et al.*, Phys. Rev. Lett. **25**, 38 (1970).
 - [2] *Nuclear Structure of the Zirconium Region*, edited by J. Erbeth, R. A. Meyer, and K. Sistemich (Springer-Verlag, Berlin, 1988).
 - [3] G. Lhersonneau *et al.*, Z. Phys. A **337**, 143 (1990).
 - [4] W. Urban *et al.*, Nucl. Phys. **A689**, 605 (2001).
 - [5] G. Lhersonneau *et al.*, Phys. Rev. C **49**, 1379 (1994).
 - [6] M. Anselment *et al.*, Z. Phys. A **326**, 493 (1987).
 - [7] D. A. Eastham *et al.*, Phys. Rev. C **36**, 1583 (1987).
 - [8] R. E. Silverans *et al.*, Phys. Rev. Lett. **60**, 2607 (1988).
 - [9] F. Buchinger *et al.*, Phys. Rev. C **41**, 2883 (1990).
 - [10] P. Lievens *et al.*, Phys. Lett. B **256**, 141 (1991).
 - [11] C. Thibault *et al.*, Phys. Rev. C **23**, 2720 (1981).
 - [12] H. A. Schuessler *et al.*, Phys. Rev. Lett. **65**, 1332 (1990).
 - [13] A. Nieminen *et al.*, Phys. Rev. Lett. **88**, 094801 (2002).
 - [14] J. Äystö, Nucl. Phys. **A693**, 477 (2001).
 - [15] J. M. G. Levins *et al.*, Phys. Rev. Lett. **82**, 2476 (1999).
 - [16] A. Nieminen *et al.*, Nucl. Instrum. Methods Phys. Res., Sect. A **469**, 244 (2001).
 - [17] P. Campbell *et al.*, J. Phys. G. **23**, 1141 (1997).
 - [18] G. Lhersonneau *et al.*, Phys. Rev. C **51**, 1211 (1995).
 - [19] P. Raghavan, At. Data Nucl. Data Tables **42**, 189 (1989).
 - [20] P. Pyykkö, Mol. Phys. **99**, 1617 (2001).
 - [21] H. L. Thayer *et al.* (to be published).
 - [22] G. Fricke *et al.*, At. Data Nucl. Data Tables **60**, 177 (1995).
 - [23] P. Campbell *et al.*, J. Phys. B **30**, 4783 (1997).
 - [24] W. D. Myers and K. H. Schmidt, Nucl. Phys. **A410**, 61 (1983).
 - [25] S. Raman *et al.*, At. Data Nucl. Data Tables **36**, 1 (1987).
 - [26] E. W. Otten, *Treatise on Heavy-Ion Science* (Plenum Press, New York, 1988), Vol. 8, p. 517.
 - [27] H. Mach *et al.*, Nucl. Phys. **A523**, 197 (1991).
 - [28] F. Buchinger *et al.*, Nucl. Phys. **A462**, 305 (1987).
 - [29] G. A. Lalazissis, S. Raman, and P. Ring, At. Data Nucl. Data Tables **71**, 1 (1999).
 - [30] P. Möller *et al.*, At. Data Nucl. Data Tables **59**, 185 (1995).